

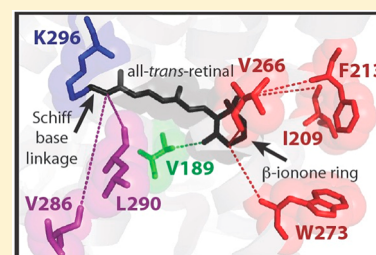
# Comparative Mutagenesis Studies of Retinal Release in Light-Activated Zebrafish Rhodopsin Using Fluorescence Spectroscopy

J. M. Morrow<sup>†</sup> and B. S. W. Chang<sup>\*,†,‡,§</sup>

<sup>†</sup>Department of Cell & Systems Biology, <sup>‡</sup>Department of Ecology & Evolutionary Biology, and <sup>§</sup>Centre for the Analysis of Genome Evolution and Function, University of Toronto, Toronto, Ontario M5S 3G5, Canada

## Supporting Information

**ABSTRACT:** Rhodopsin is the visual pigment responsible for initiating scotopic (dim-light) vision in vertebrates. Once activated by light, release of all-*trans*-retinal from rhodopsin involves hydrolysis of the Schiff base linkage, followed by dissociation of retinal from the protein moiety. This kinetic process has been well studied in model systems such as bovine rhodopsin, but not in rhodopsins from cold-blooded animals, where physiological temperatures can vary considerably. Here, we characterize the rate of retinal release from light-activated rhodopsin in an ectotherm, zebrafish (*Danio rerio*), demonstrating in a fluorescence assay that this process occurs more than twice as fast as bovine rhodopsin at similar temperatures in 0.1% dodecyl maltoside. Using site-directed mutagenesis, we found that differences in retinal release rates can be attributed to a series of variable residues lining the retinal channel in three key structural motifs: an opening in metarhodopsin II between transmembrane helix 5 (TMS) and TM6, in TM3 near E122, and in the “retinal plug” formed by extracellular loop 2 (EL2). The majority of these sites are more proximal to the  $\beta$ -ionone ring of retinal than the Schiff base, indicating their influence on retinal release is more likely due to steric effects during retinal dissociation, rather than alterations to Schiff base stability. An Arrhenius plot of zebrafish rhodopsin was consistent with this model, inferring that the activation energy for Schiff base hydrolysis is similar to that of bovine rhodopsin. Functional variation at key sites identified in this study is consistent with the idea that retinal release might be an adaptive property of rhodopsin in vertebrates. Our study is one of the few investigating a nonmammalian rhodopsin, which will help establish a better understanding of the molecular mechanisms contributing to vision in cold-blooded vertebrates.



Rhodopsin, a member of the G protein-coupled receptor (GPCR) superfamily, is the visual pigment responsible for mediating the critical first step of dim-light vision in vertebrates.<sup>1</sup> The 11-*cis*-retinal chromophore is bound through a protonated Schiff base linkage at K296<sup>2</sup> and serves as a strong inverse agonist, maintaining stability and greatly reducing thermal activation of dark state rhodopsin.<sup>3</sup> Upon activation, 11-*cis*-retinal is converted to its stereoisomer, all-*trans*-retinal, resulting in a series of conformational changes in rhodopsin, including the metarhodopsin II (meta II) state, which activates the G protein transducin.<sup>4</sup> Within milliseconds of formation, meta II is subjected to a two-step deactivation process, comprising C-terminal phosphorylation followed by arrestin binding, quenching the catalytic activity of the activated state.<sup>5</sup> For rhodopsin to regenerate *in vivo* following activation, all-*trans*-retinal must be released, involving hydrolysis of the existing Schiff base link and dissociation of free retinal from opsin. This allows new 11-*cis*-retinal to enter the chromophore binding pocket to form a Schiff base link with opsin, restoring photosensitivity.<sup>6,7</sup>

In recent years, bovine rhodopsin crystal structures of the dark state,<sup>8</sup> open pocket,<sup>9</sup> and activated state<sup>10</sup> have revealed a number of unexpected features relevant to chromophore regeneration and release. The dark state crystal structure was found to contain a  $\beta$ -sheet consisting of strands from extracellular loop 2 (EL2), effectively plugging the extracellular opening in rhodopsin,<sup>8,11</sup> and blocking what was believed to be

one of the possible access sites of retinal. Further investigation suggested the possibility of a channel within the transmembrane domains that would facilitate the travel of retinal to and from the chromophore binding pocket, along with terminal binding sites for retinal on the surface of rhodopsin.<sup>12,13</sup> Crystal structures for the chromophore-free,<sup>9</sup> G protein-interacting,<sup>14</sup> and meta II<sup>10</sup> states of rhodopsin confirmed the existence of two transmembrane openings on opposite sides of rhodopsin that open into the hydrophobic membrane layer: one between transmembrane helix 1 (TM1) and TM7, and one between TMS and TM6.<sup>15</sup> The latter opening is a good candidate for the site of retinal release, considering the outward rotation of TM6 following activation.<sup>16,17</sup> Molecular dynamics simulations have shown the possibility of retinal exiting through this opening, led by its  $\beta$ -ionone ring.<sup>18</sup> Recent mutagenesis studies have primarily attributed changes in the rate of retinal release to either Schiff base stability<sup>19</sup> or retinal dissociation,<sup>20</sup> suggesting that conflicting ideas currently exist regarding the dominant mechanism mediating this kinetic rate. These studies utilized fluorescence spectroscopy to monitor retinal release,<sup>19,20</sup> and an Arrhenius plot based on this data was used to infer the

Received: November 5, 2014

Revised: June 15, 2015

activation energy of Schiff base hydrolysis to evaluate changes in Schiff base stability.<sup>20</sup> While these studies examined the contributions of conserved sites in rhodopsin, as well as differences between rod and cone opsins, the mechanisms that underlie natural variation in retinal release rates among vertebrate rhodopsins have yet to be investigated.

Despite being one of the most extensively studied members of the GPCR superfamily, the vast majority of kinetic studies of rhodopsin function have utilized bovine and other model mammalian rhodopsins (e.g., ref 21), or chicken rhodopsin (e.g., ref 22). One of the few studies to examine retinal release in a nonmodel organism, the echidna, suggests that variation in kinetic rates exists among mammalian rhodopsins,<sup>23</sup> even if the differences are more subtle than those between rhodopsin and cone opsins.<sup>20</sup> This is not surprising considering that other functional differences among rhodopsins have also been reported, including hydroxylamine stability,<sup>24</sup> and kinetics of metarhodopsin intermediates.<sup>25,26</sup> An ectotherm, like zebrafish, is an ideal candidate to highlight natural differences in rhodopsin function relative to endothermic mammals, since kinetic processes have likely adapted to function at variable physiological temperatures in cold blooded animals. Additionally, zebrafish is a well-studied model for the vertebrate visual system, where increased understanding of rhodopsin structure and function may reveal insight into visual development, as well as behavior and physiology.<sup>27–29</sup> Since it has been suggested that the rate of retinal release may influence dark adaptation at low bleaching levels,<sup>30</sup> investigating the molecular mechanisms of retinal release in rhodopsin could also help to better understand variability in dim-light vision among vertebrates.

Here, we investigate the natural variation in the rate of retinal release between zebrafish and bovine rhodopsin using an assay that monitors how the intrinsic fluorescence of opsin becomes unquenched upon release of retinal from the chromophore binding pocket. Amino acid differences between these rhodopsins were identified, and a series of zebrafish rhodopsin mutants substituting bovine rhodopsin identities at variable sites were made. We found that zebrafish rhodopsin released retinal more than twice as fast as bovine rhodopsin, with this discrepancy being mainly attributable to the rate of dissociation of retinal from opsin as opposed to differences in Schiff base stability, since variation at functional motifs proximal to the  $\beta$ -ionone ring of retinal were found to be responsible for most of this difference. Additionally, an Arrhenius plot of zebrafish rhodopsin suggested that a similar energy of activation is required to hydrolyze the Schiff base as compared to bovine rhodopsin. This study also reinforces the importance of sites 122 and 189 on the stability of metarhodopsin intermediates, as substitutions that influenced the positioning of these sites in the chromophore binding pocket also affected retinal release. This is the first time that all-*trans*-retinal release has been investigated in a fish rhodopsin.

## ■ EXPERIMENTAL PROCEDURES

**Visual Pigment Expression and Purification.** RNA was extracted from adult zebrafish eyes using TRIzol (Invitrogen), and cDNA libraries were made using the SMART cDNA Library Construction Kit (BD Biosciences). Zebrafish rhodopsin has a coding sequence of 1,065 bp, translating to 354 amino acids. This includes 59 differences from bovine rhodopsin, along with 6 additional residues in the C-terminal domain (Figure S1). The complete coding sequence of zebrafish rhodopsin (GenBank: AB087811) was amplified using

PfuTurbo (Stratagene) and inserted into the pJET1.2 cloning vector (Fermentas). Site-directed mutagenesis primers were designed to induce single amino acid substitutions, with double and triple mutants being generated through successive rounds of mutagenesis via PCR. All sequences were verified using a 3730 DNA Analyzer (Applied Biosystems). The full length coding sequence of bovine rhodopsin<sup>31</sup> was cloned into the pIRES-hrGFP II expression vector (Stratagene), while zebrafish rhodopsin and mutants were cloned into the p1D4-hrGFP II expression vector.<sup>32</sup> These constructs were used to transiently transfect cultured HEK293T cells using Lipofectamine 2000 (Invitrogen). Cells were harvested 48 h post-transfection and opsins were regenerated using 11-*cis*-retinal, generously provided by Dr. Rosalie Crouch (Medical University of South Carolina). Visual pigments were solubilized in 1% *N*-dodecyl- $\beta$ -maltoside (DM) and immunoaffinity purified using the 1D4 monoclonal antibody,<sup>33</sup> as previously described.<sup>32,34</sup> Purified visual pigment samples were eluted in sodium phosphate buffer (50 mM NaPhos, 0.1% DM, pH 7).

**Spectroscopy.** The ultraviolet–visible absorption spectra of purified zebrafish, bovine, and mutant rhodopsins were recorded at 25 °C using a Cary 4000 double-beam spectrophotometer (Agilent). All  $\lambda_{\text{MAX}}$  values were calculated after fitting absorbance spectra to a standard template for A1 visual pigments.<sup>35</sup> Activation of zebrafish rhodopsin in response to light was measured by a shift in  $\lambda_{\text{MAX}}$  to  $\sim$ 380 nm, representing the active meta II state. Reactivity to hydroxylamine in the dark was monitored by absorbance spectroscopy upon incubation in 50 mM  $\text{NH}_2\text{OH}$  (Sigma-Aldrich) at 25 °C. Acid denaturation was similarly monitored upon incubation in 100 mM HCl (Sigma-Aldrich). Retinal release following rhodopsin light activation was monitored using a Cary Eclipse fluorescence spectrophotometer equipped with a Xenon flash lamp (Agilent), according to a protocol modified from a previous study.<sup>36</sup> Briefly, 0.1–0.2  $\mu\text{M}$  visual pigment samples were bleached for 30 s with a fiber optic lamp (Dolan-Jenner), using a filter to restrict wavelengths of light below 475 nm to minimize heat. Fluorescence measurements were obtained at 30 s intervals with a 2 s integration time. The excitation wavelength was 295 nm (1.5 nm slit width), and the emission wavelength was 330 nm (10 nm slit width); no noticeable activation by the excitation beam was detected prior to pigment bleaching. Retinal release resulted in decreased quenching of intrinsic tryptophan fluorescence at W265 by the retinal chromophore.<sup>36</sup> Data was fit to a three variable, first order exponential equation ( $y = y_0 + a(1 - e^{-bx})$ ), with half-life values calculated based on the rate constant  $b$  ( $t_{1/2} = \ln 2/b$ ). All curve fitting resulted in  $r^2$  values of greater than 0.95. While zebrafish rhodopsin has an additional tryptophan compared to bovine rhodopsin (W273), it should not have a significant influence on fluorescence quenching considering its distance from the chromophore. Differences in retinal release half-life values were assessed using a two-tailed  $t$  test with unequal variance. All data for mutant rhodopsins were recorded at 20 °C, while additional data for wild type rhodopsins used to construct Arrhenius plots was also collected at 5 °C, 18 °C, and 24 °C. Bovine rhodopsin was also assayed at 37 °C, representing its physiological temperature. Activation energies ( $E_a$ ) were determined based on the Arrhenius equation ( $k = A e^{-E_a/(RT)}$ ) and calculated from the slope of a linear regression line fit to a plot of the natural logarithm of retinal release rate constants against the reciprocals of these temperatures.<sup>20,37</sup>

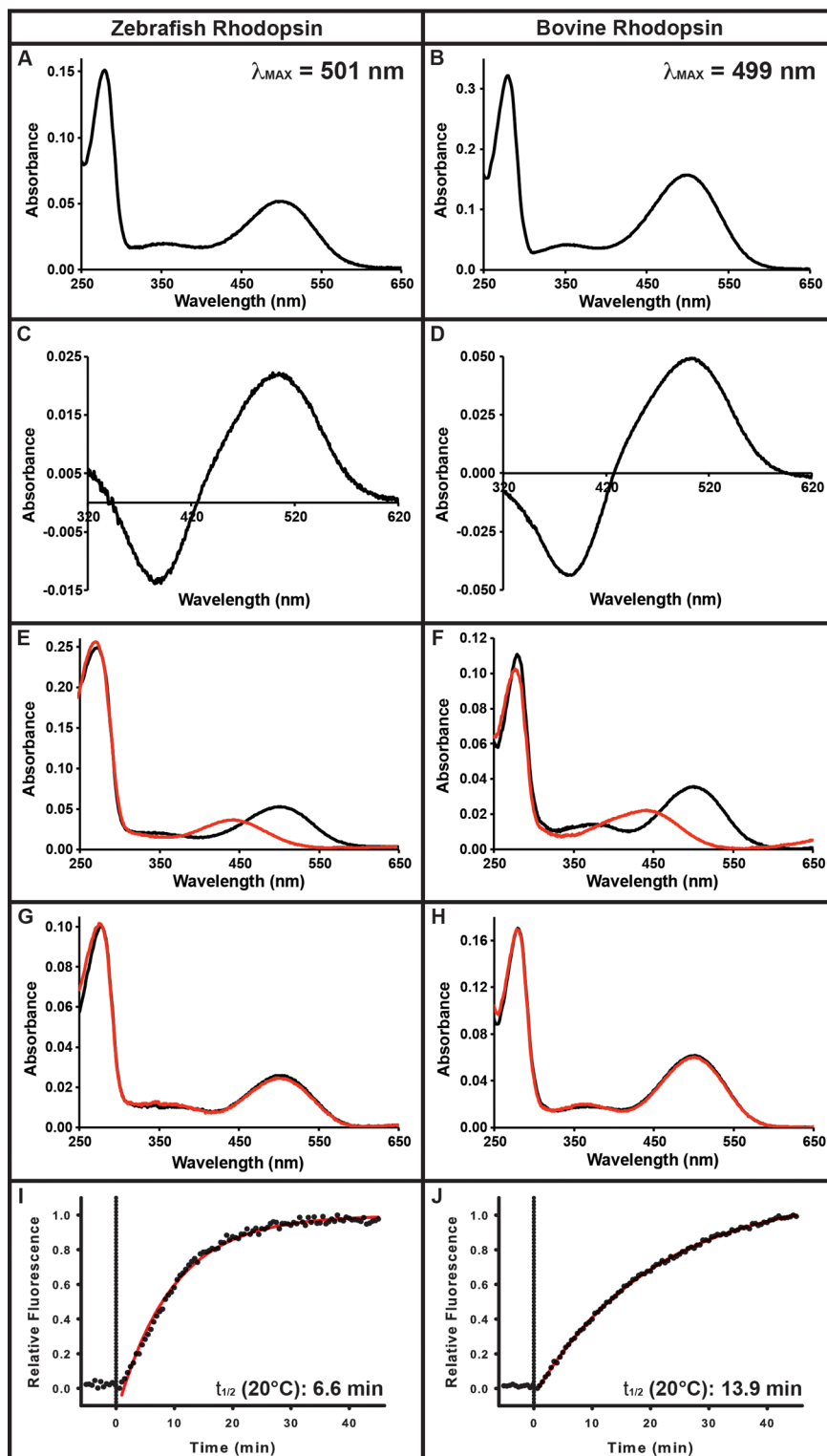


**Figure 1.** Spectroscopic comparison of zebrafish and bovine rhodopsin. (A,B) Ultraviolet-visible absorbance spectra of zebrafish and bovine rhodopsin, respectively, following *in vitro* expression and purification. The wavelength of maximum absorbance ( $\lambda_{MAX}$ ) is indicated for each pigment. (C,D) Difference spectra of zebrafish and bovine rhodopsin, respectively, calculated by subtracting the light-bleached absorption spectrum from the dark spectrum, showing a shift from  $\lambda_{MAX}$  to  $\sim 380$  nm following photoactivation. (E,F) Absorption spectra of zebrafish and bovine rhodopsin, respectively, both before (black) and after (red) incubation in 100 mM HCl. A shift from  $\lambda_{MAX}$  to  $\sim 440$  nm demonstrates a covalent Schiff base linkage between opsin and chromophore. (G-H) Absorption spectra of zebrafish and bovine rhodopsin, respectively, both before (black) and after (red) incubation in 50 mM  $NH_2OH$  for 2 h. No difference following incubation suggests a chromophore binding pocket that is inaccessible to small molecules, such as  $NH_2OH$ . (I,J) Increase in fluorescence intensity, representing release of all-*trans*-retinal from the chromophore binding pocket, in zebrafish and bovine rhodopsin, respectively, following photoactivation at  $t = 0$  (dotted line). Half-life values of the first-order kinetic reactions are indicated. Samples were assayed at 20 °C, pH 7.0, in 0.1% dodecyl maltoside.

**Homology Modeling.** The 3D structure of zebrafish rhodopsin was inferred via homology modeling by Modeller,<sup>38,39</sup> using the bovine meta II crystal structure (PDB code: 3PQR<sup>9</sup>) as template, including chromophore and water molecules. Minimizing the Modeller objective function generated 25 separate models, and the run with the lowest DOPE score was assessed and visualized.<sup>40</sup> ProCheck was used to ensure bond angles and lengths were generally in high probability stereochemical conformations as indicated by positive overall *G*-factor.<sup>41</sup> Model quality was further examined by ProSA-web by comparing the model's total energy to that expected by random chance.<sup>42</sup> Our model and template structures had comparable *z*-scores, standardized for the number of residues. Images of 3D structures were generated using MacPyMol.<sup>43</sup>

## RESULTS

**Zebrafish Rhodopsin Has an Increased Rate of Retinal Release Compared to Bovine Rhodopsin at Similar Temperatures.** Both zebrafish and bovine rhodopsin were expressed, regenerated with 11-*cis*-retinal, and purified, producing dark spectra with  $\lambda_{\text{MAX}}$  of 501 and 499 nm, respectively (Figure 1A,B). These values are similar to previously published results,<sup>44,45</sup> and are consistent with  $\lambda_{\text{MAX}}$  values from the majority of vertebrates, which are generally around 500 nm.<sup>46,47</sup> When photoactivated, the  $\lambda_{\text{MAX}}$  of zebrafish rhodopsin shifts to  $\sim 380$  nm, characteristic of the biologically active meta II intermediate and similar to bovine rhodopsin (Figure 1C,D). Confirmation of a covalent Schiff base linkage between zebrafish rhodopsin and its 11-*cis*-retinal chromophore was shown by a shift in  $\lambda_{\text{MAX}}$  to 440 nm following denaturation with acid, the typical absorbance maximum of 11-*cis*-retinal bound to denatured opsin (Figure 1E,F). Zebrafish rhodopsin was not initially susceptible to hydroxylamine (Figure 1G), suggesting it has chromophore binding pocket accessibility similar to that of bovine rhodopsin (Figure 1H), which also shows no significant reaction over an extended period of time.<sup>24</sup> In a fluorescence assay monitoring for release of all-*trans*-retinal, light-activated bovine rhodopsin had a half-life ( $t_{1/2}$ ) of  $13.9 \pm 1.6$  min, similar to previously recorded values of 12.5–15.5 min.<sup>36,48</sup> However, under similar conditions, zebrafish rhodopsin was found to have a significantly shorter half-life of  $6.6 \pm 0.6$  min (Figure 1I,J; Table 1). To further investigate this functional difference, we conducted mutagenesis of sites lining the retinal channel of rhodopsin, as well as those surrounding terminal openings of this channel. We replaced variable sites in zebrafish rhodopsin with corresponding bovine identities in order to determine which sites were responsible for the observed differences in retinal release rates (Table 1).

**Amino Acid Substitutions at Variable Sites near the Chromophore Alter Retinal Release.** The substitution with the largest effect on the rate of retinal release in this study was M123I ( $t_{1/2} = 11.5 \pm 0.7$  min), resulting in a half-life almost 5 min longer than that of wild type zebrafish rhodopsin (Table 1, Figure 2A). This is a residue in TM3 within 8 Å of the  $\beta$ -ionone ring end of the retinal chromophore in the binding pocket.<sup>8,11</sup> Mutagenesis at a neighboring residue, G124A, also resulted in a longer half-life ( $t_{1/2} = 8.4 \pm 0.5$  min), although not as pronounced as that of M123I (Figure 2B). However, the double mutant M123I/G124A had an intermediate phenotype relative to the two individual substitutions ( $t_{1/2} = 10.6 \pm 1.6$  min), which suggests that these substitutions are affecting the

**Table 1. Retinal Release Half-Life, and  $\lambda_{\text{MAX}}$  Values for Wild Type and Mutant Rhodopsins, Measured at 20 °C**

opsin	retinal release $t_{1/2}$ (min) <sup>a</sup>	difference from WT zebrafish rhodopsin (min) <sup>b</sup>	$\lambda_{\text{MAX}}$ (nm)
bovine rhodopsin	$13.9 \pm 1.6$ (19)		499
zebrafish rhodopsin	$6.6 \pm 0.6$ (54)		501
A33E	$6.5 \pm 0.1$ (3)		500
A36Q	$7.0 \pm 0.6$ (3)		501
E64Q	$7.0 \pm 0.4$ (3)		501
M95L	$6.9 \pm 0.7$ (3)		501
R107P	$5.9 \pm 1.1$ (3)		501
M123I	$11.5 \pm 0.7$ (5)	+4.9**	501
G124A	$8.4 \pm 0.5$ (3)	+1.8*	501
W136Y	$7.1 \pm 0.3$ (4)		500
C165L	$5.7 \pm 0.4$ (3)	−0.9*	501
V189I	$9.1 \pm 0.9$ (4)	+2.5**	500
I209V	$5.3 \pm 0.7$ (3)	−1.3*	500
F213I	$8.1 \pm 0.6$ (9)	+1.5**	500
R225Q	$5.8 \pm 0.7$ (3)		502
E241A	$6.0 \pm 0.5$ (3)		500
R248K	$7.1 \pm 0.8$ (4)		500
V266L	$8.3 \pm 0.3$ (5)	+1.7**	499
W273F	$8.8 \pm 0.8$ (7)	+2.2**	499
V286I	$5.7 \pm 0.3$ (3)	−0.9**	501
L290I	$5.3 \pm 0.5$ (3)	−1.3*	500
C304V	$6.6 \pm 0.4$ (3)		501
C308M	$6.9 \pm 0.5$ (3)		500
H315N	$6.9 \pm 0.6$ (3)		501
M123I, G124A	$10.6 \pm 1.6$ (6)	+4.0**	502
F213I, V266L	$11.1 \pm 0.4$ (3)	+4.5**	500
F213I, W273F	$10.1 \pm 0.9$ (5)	+3.5**	499
V266L, W273F	$10.0 \pm 1.0$ (8)	+3.4**	498
F213I, V266L, W273F	$13.3 \pm 0.6$ (4)	+6.7**	498
I209 V, F213I, V266L, W273F	$13.1 \pm 1.0$ (3)	+6.5**	497

<sup>a</sup>For retinal release half-life values, the number of replicates are indicated in brackets. <sup>b</sup>Significant differences from wild type zebrafish rhodopsin are indicated, based on a two-tailed *t* test with unequal variance, where  $p < 0.05$  (\*) or  $< 0.01$  (\*\*).

chromophore indirectly, possibly by repositioning a nearby residue with a more direct influence (Figure 2C). A likely candidate is the neighboring E122, a determinant of opsin function previously shown to mediate decay rates of metarhodopsin intermediates.<sup>49,50</sup> Homology models of zebrafish rhodopsin confirm the proximity of E122 to the  $\beta$ -ionone ring of the chromophore, similar to bovine rhodopsin. Since E122 is a charged residue, it is possible that its repositioning could modify the hydrostatic environment of the binding pocket and its hydrogen bonding network.<sup>51,52</sup> Other substitutions less proximal to E122 had no significant effects on retinal release rates, including R107P and W136Y. The latter result was somewhat surprising, as Y136 is highly conserved in most rhodopsin-like Family A GPCRs as the third residue of the D(E)RY motif, which has previously been shown to be relevant to rhodopsin activation.<sup>53,54</sup>

Separating the retinal channel of rhodopsin from the extracellular environment is a  $\beta$ -sheet structure formed by  $\beta$ -strands from EL2, where strand  $\beta 4$ , consisting of sites 186–190, lines the chromophore binding pocket.<sup>8,55</sup> Site 189 is a known determinant of rod and cone opsin function<sup>22</sup> that also varies

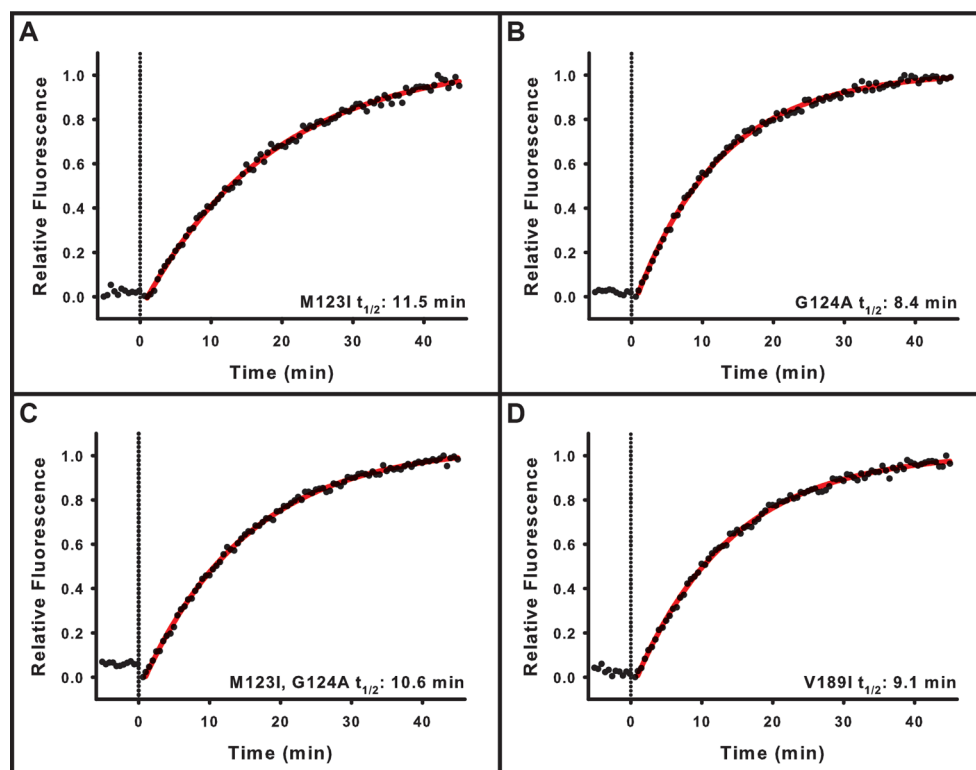


**Figure 2.** Increase in fluorescence intensity following photoactivation of zebrafish rhodopsin mutants, with substitutions to bovine rhodopsin identities at residues lining the chromophore binding pocket. Mutants include (A) M123I, (B) G124A, (C) M123I/G124A, and (D) V189I. Half-life values of the first-order kinetic reactions are indicated. Photoactivation occurred at  $t = 0$  (dotted line). Samples were assayed at 20 °C, pH 7.0, in 0.1% dodecyl maltoside.

between valine and isoleucine among rhodopsins. The V189I substitution in zebrafish rhodopsin significantly decreased the rate of retinal release ( $t_{1/2} = 9.1 \pm 0.9$  min; Figure 2D). In bovine rhodopsin, I189 is only a few angstroms away from the chromophore, and homology modeling suggests this is also the case for V189 in zebrafish rhodopsin.

#### Variable Residues near an Opening between TM5 and TM6 in Meta II Contribute to Retinal Release Rate Differences between Zebrafish and Bovine Rhodopsin.

The opening located between TMS and TM6 in meta II has been hypothesized as the site of all-*trans*-retinal release following photoactivation.<sup>12,15</sup> In bovine rhodopsin, key residues at this motif, including a triad of phenylalanines at 208, 273, and 276, form a “hydrophobic cage” that could sterically hinder the release of all-*trans*-retinal.<sup>10,18</sup> We investigated substitutions near this opening in zebrafish rhodopsin and measured their impact on retinal release rates. The largest difference was caused by W273F, also the substitution most proximal to the opening, which decreased the rate of retinal release ( $t_{1/2} = 8.8 \pm 0.8$  min). Three additional substitutions nearby also had minor effects on retinal release rates: I209V, F213I, and V266L (Figure 3A–D). Other substitutions less proximal to the opening (R225Q, E241A, and R248K) had no discernible effects (Table 1). A quadruple mutant (I209V, F213I, V266L, W273F) was also generated to determine whether the influence of these residues was additive; this mutant caused a much larger decrease in the rate of retinal release relative to the individual substitutions ( $t_{1/2} = 13.1 \pm 1.0$  min; Figure 3E). With the exception of W273, side chains of these residues might have little direct contact with the chromophore during release, but they could be involved

indirectly by altering the orientation of surrounding residues. These substitutions likely influence steric effects during all-*trans*-retinal dissociation as opposed to Schiff base stability, due to their proximity to the  $\beta$ -ionone ring and the hypothesized retinal exit site. A triple reverse mutant (I213F, L266V, F273W) was also generated in bovine rhodopsin, confirming that the effect of these substitutions is consistent in both backgrounds (Supporting Information Table S2).

We also investigated substitutions near another channel opening, located between TM1 and TM7, that is closer to the Schiff base link than the previous opening, and is formed during activation when the backbone of F293 in TM7 rotates 120°.<sup>9,10</sup> Overall, the effects of substitutions at this opening were much less compared to those at the TMS/TM6 opening. V286I and L290I caused minor changes to retinal release rates, likely due to their proximity to either the Schiff base or to F293 (Figure 3F,G), while A36Q and C304V had no significant effect (Table 1).

#### Zebrafish and Bovine Rhodopsin Have Similar Activation Energies of Schiff Base Hydrolysis.

Additional temperatures were assayed for wild type zebrafish and bovine rhodopsin in order to construct an Arrhenius plot to estimate activation energies of Schiff base hydrolysis (Table 2). Interestingly, the activation energies for zebrafish rhodopsin ( $18.2 \pm 1.7$  kcal/mol) and bovine rhodopsin ( $19.2 \pm 1.3$  kcal/mol) were found to be quite similar (Figure 4). These values are similar not only to previously measured activation energies of bovine rhodopsin, but also of the *Xenopus* SWS1 visual pigment.<sup>20</sup> This suggests that Schiff base stability may only make a minor contribution to differences in retinal release among these visual pigments. This result is consistent with our

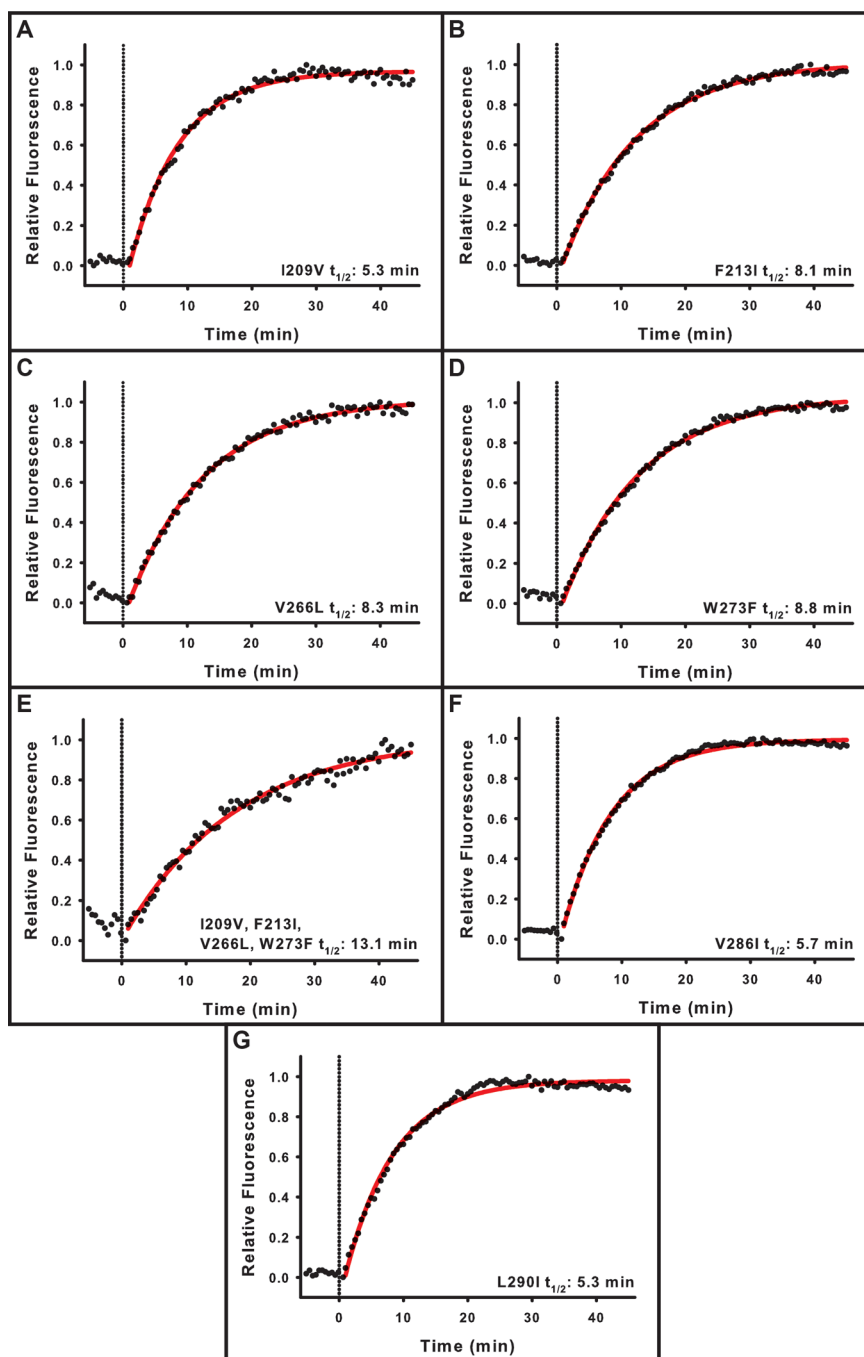


**Figure 3.** Increase in fluorescence intensity following photoactivation of zebrafish rhodopsin mutants, with substitutions to bovine rhodopsin identities at residues near two openings in metarhodopsin II. Mutants include (A) I209V, (B) F213I, (C) V266L, (D) W273F, (E) I209V/F213I/V266L/W273F, (F) V286I, and (G) L290I. Half-life values of the first-order kinetic reactions are indicated. Photoactivation occurred at  $t = 0$  (dotted line). Samples were assayed at 20 °C, pH 7.0, in 0.1% dodecyl maltoside.

mutagenesis data, in which the majority of amino acid substitutions with significant effects on retinal release were located closer to the  $\beta$ -ionone ring, rather than the Schiff base of the chromophore. These sites would therefore be more likely to sterically hinder the dissociation of retinal from rhodopsin, following Schiff base hydrolysis.

The rate of retinal release of zebrafish rhodopsin is significantly increased compared to that of bovine rhodopsin at similar temperatures, resulting in a half-life that is more than two times shorter. However, zebrafish is an ectotherm whose body temperature is dependent on its environment. This is in

contrast to homeothermic mammals, whose body temperatures are usually around 37 °C. The natural habitat of the zebrafish is found mainly in the Ganges and Brahmaputra river basins in India, Bangladesh, and Nepal.<sup>56</sup> Temperatures in these rivers usually vary between 17 and 27 °C depending on the time of year;<sup>57</sup> therefore, assaying zebrafish rhodopsin within this range would be a better approximation of physiological temperatures. When measured at more physiologically relevant temperatures, the retinal release rate of zebrafish rhodopsin ( $t_{1/2} = 4.1 \pm 0.6$  min at 24 °C; Figure 4E) was found to be more similar that of bovine rhodopsin ( $t_{1/2} = 2.0 \pm 0.2$  min at 37 °C; Figure S2).

**Table 2. Retinal Release Half-Life Values of Wild Type Bovine and Zebrafish Rhodopsin Compared at Different Temperatures**

visual pigment	T (°C)	$t_{1/2}$ (min) <sup>a</sup>
bovine rhodopsin	5	70.7 ± 4.3 (3)
	18	19.7 ± 1.2 (4)
	20	13.9 ± 1.6 (19)
	24	8.6 ± 1.0 (4)
	37	2.0 ± 0.2 (7)
zebrafish rhodopsin	5	35.7 ± 2.6 (2)
	18	10.5 ± 1.6 (4)
	20	6.6 ± 0.6 (54)
	24	4.1 ± 0.6 (4)

<sup>a</sup>For retinal release half-life values, the number of replicates are indicated in brackets.

This implies that even though bovine rhodopsin has a decreased rate of retinal release compared to zebrafish rhodopsin when measured at similar temperatures in the lab, it may in fact release retinal at a more comparable rate to zebrafish rhodopsin *in vivo*, and that these differences are driven by amino acid substitutions at nonconserved sites.

**Amino Acid Substitutions at Variable Sites That Alter Retinal Release Do Not Change  $\lambda_{MAX}$ .** Spectral tuning (changes to  $\lambda_{MAX}$ ) has been the focus of most comparative studies of visual pigment function,<sup>58–61</sup> while relatively few studies highlight other aspects of visual pigment function in a comparative context.<sup>23,24,62</sup> In contrast, our study targeted sites differing between zebrafish and bovine rhodopsin that line the retinal channel and its terminal openings, and found very little effect on  $\lambda_{MAX}$  despite the proximity of some of the sites to the chromophore (Table 1).

## DISCUSSION

This study investigated the effects of natural variation in zebrafish and bovine rhodopsin on the rate of light-activated retinal release using site-directed mutagenesis and fluorescence spectroscopy. We found that the retinal release rate of zebrafish rhodopsin is significantly increased compared to that of bovine rhodopsin at similar temperatures, and have highlighted several known structural motifs lining a previously identified retinal channel<sup>9,15</sup> where natural sequence variation is capable of tuning retinal release rates (Figure 5). However, we also found that the energy of activation required to hydrolyze the Schiff base in zebrafish rhodopsin, inferred through an Arrhenius plot of retinal release data, seems comparable to that of bovine rhodopsin.<sup>20</sup> Under the assumption that the activation energy of Schiff base hydrolysis is related to Schiff base stability, and when combined with *a priori* crystal structure information concerning the positions of variable sites near the chromophore in metarhodopsin II,<sup>10</sup> our results suggest that all-*trans*-retinal dissociation, and not Schiff base stability, is more likely to be the molecular mechanism that primarily mediates retinal release differences among rhodopsins. Additionally, bovine rhodopsin was found to release retinal more comparably to zebrafish rhodopsin at their respective physiological temperatures, implying that there is a possibility that sequence evolution affecting retinal release rates may be tuning this kinetic process as an adjustment to temperature. Here, we discuss the importance of our findings for the understanding of molecular mechanisms mediating retinal release and their implications for the vertebrate visual system.

Recently, two key studies have also investigated the molecular mechanisms responsible for mediating retinal release. One performed site-directed mutagenesis at highly conserved sites around both retinal channel openings in bovine rhodopsin.<sup>19</sup> Significant differences were shown for both retinal uptake and release in many of these mutants, leading to the conclusion that these substitutions were altering the stability of the Schiff base linkage. The authors argued that local steric effects of amino acid side chains alone could not explain why a single substitution would change rates of both retinal uptake and release. Another study used bovine rhodopsin and a short wavelength-sensitive cone opsin from *Xenopus* (VCOP) to explore the differences between retinal release in rod and cone opsins.<sup>20</sup> While release from VCOP occurred 250 times faster than in bovine rhodopsin, Arrhenius plots suggested that activation energies in both visual pigments were remarkably similar. With comparable energetics for Schiff base hydrolysis, the authors concluded that steric interactions of all-*trans*-retinal with side chains during release was the likely mechanism to explain differences in retinal release rates between rod and cone opsins. Our mutagenesis results support the idea of steric effects being of primary importance for mediating differences in retinal release rates between bovine and zebrafish rhodopsins, since our study showed that the majority of sites that altered release rates were found closer to the  $\beta$ -ionone ring of retinal than to the Schiff base. This is also consistent with our data from Arrhenius plots of zebrafish and bovine rhodopsin, which suggest a comparable energy of activation. However, it is also clear that Schiff base stability can have important effects on retinal release rates, as was shown when highly conserved residues responsible for establishing core structural stability in rhodopsin were mutated.<sup>19</sup> It also appears that substitutions in our study that have a larger effect on retinal release rates, such as 123 and 273, occur at more invariant sites, while those showing more naturally occurring variation, such as 213 and 290, cause smaller changes (Figure S3).

Additionally, it was interesting to see that retinal release in zebrafish rhodopsin was comparable to that found in bovine rhodopsin when both were assayed closer to their physiological temperatures. This may hint at evolutionary adaptations in rhodopsins of homeothermic vertebrates that slow down kinetic reactions in order to compensate for higher ambient temperatures. A previous study described how the decay of meta II to meta III in human rhodopsin is faster than in bovine rhodopsin.<sup>26</sup> While retinal release comprises more than just meta II decaying to meta III, measuring retinal release at physiological temperatures in other mammals, such as humans, would be required to better understand this relationship. This association with temperature could also apply to other kinetic processes of visual pigments, including the lumirhodopsin<sup>63</sup> and metarhodopsin equilibria.<sup>26,64</sup> This may be important as changes to the metarhodopsin equilibrium due to temperature can subsequently vary rates of G protein activation.<sup>65</sup> Intriguingly, there is even evidence in *Drosophila* that rhodopsin is involved in thermotactic discrimination to help locate settings of ideal temperature,<sup>66</sup> further supporting a fundamental connection between G protein visual function and temperature. Much of this association is likely rooted in the steep dependence observed between temperature and dark state Schiff base hydrolysis,<sup>67</sup> as the hydrogen bond network surrounding the Schiff base is known to be important in mediating critical interactions that can change the activation energy of hydrolysis.<sup>68</sup>

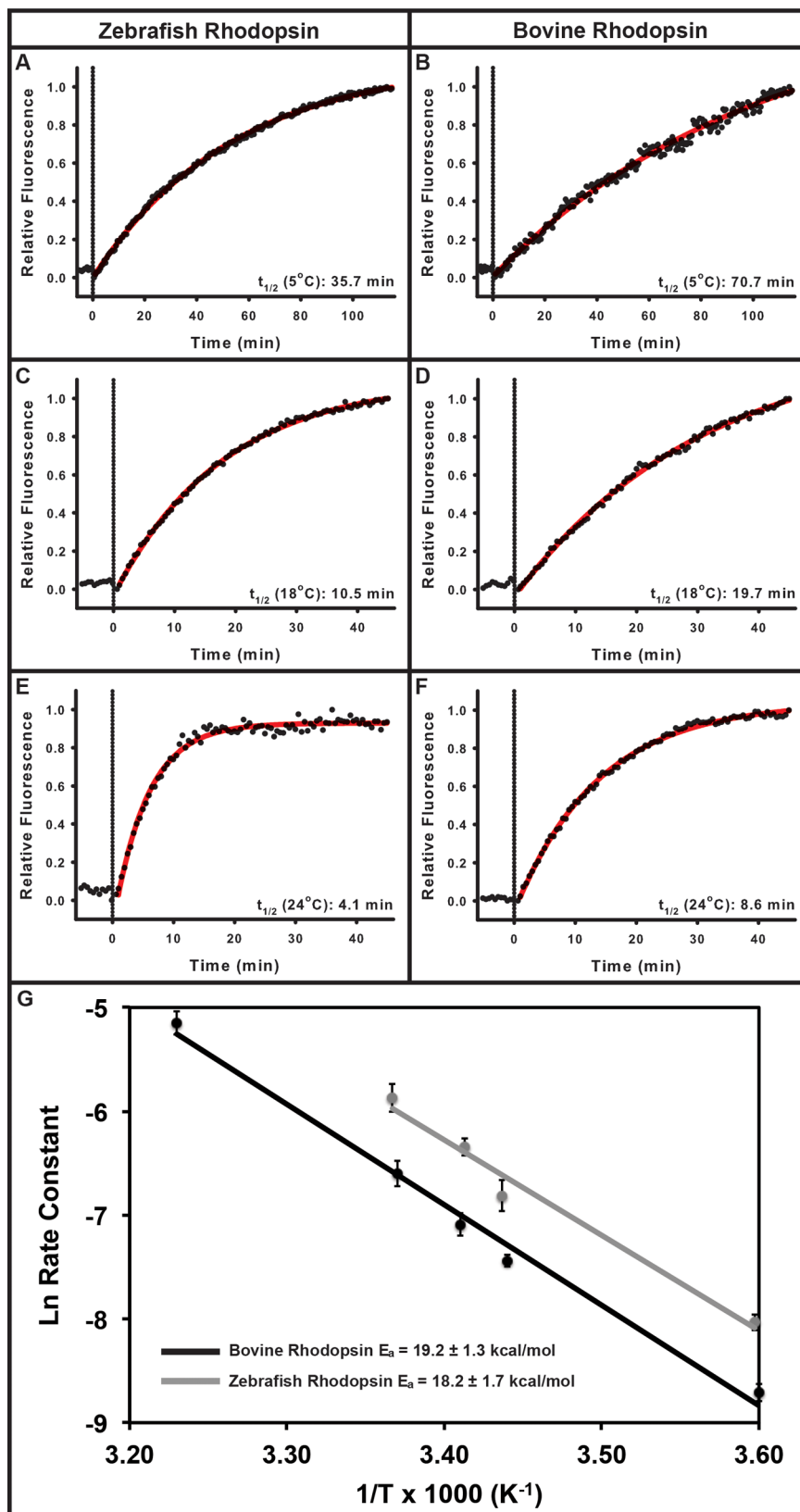


**Figure 4.** Comparison of retinal release of zebrafish and bovine rhodopsin at varying temperatures. (A–F) Retinal release half-life values were calculated between 5 and 37 °C at pH 7.0 by measuring the increase in fluorescence intensity following photoactivation at  $t = 0$  (dotted line). (G) Arrhenius plot of the natural logarithm of the rates of fluorescence increase in photoactivated bovine (black) and zebrafish (gray) rhodopsin. Activation energies ( $E_a$ ) were estimated from the negative reciprocal of the slope of a linear regression line that best fit the data ( $r^2 > 0.97$ ). Data points indicate means and error bars represent standard deviation.

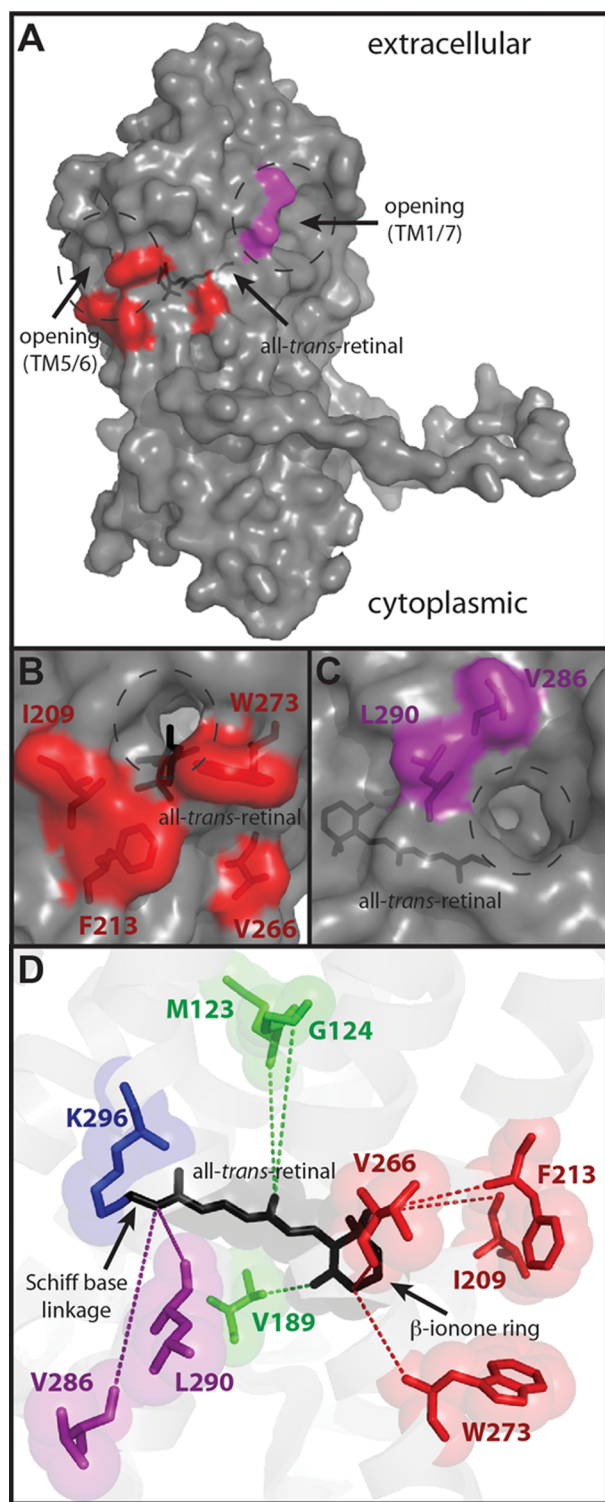


**Figure 5.** Crystal structure homology model of zebrafish metarhodopsin II, based on bovine metarhodopsin II (9). (A) Complete structure of the surface of zebrafish metarhodopsin II. Highlighted residues were mutated in this study near openings at TMs 5 and 6 (red) or TMs 1 and 7 (purple). Close up of openings in metarhodopsin II at (B) TMs 5 and 6 and (C) TMs 1 and 7 show the proximal residues mutated in this study and their positions relative to the chromophore, all-*trans*-retinal. (D) All mutations investigated in this study that significantly altered retinal release are shown in relation to all-*trans*-retinal, bound to K296 through a covalent Schiff base linkage.

This study also emphasizes the importance of studying rhodopsin natural variation. Our group recently investigated light-activated retinal release rates in echidna rhodopsin, showing that it was significantly different from bovine rhodopsin,<sup>23</sup> suggesting additional variation may exist even within mammals. In fact, although not well investigated, other studies also hint at variability in aspects of rhodopsin function other than spectral tuning. For example, hydroxylamine reactivity is known to differ markedly between rod and cone opsins, with cone opsins undergoing Schiff base hydrolysis much more rapidly upon exposure to hydroxylamine in comparison with bovine rhodopsin, which does not react.<sup>69–71</sup> However, in some cases, it has been found that there are also rhodopsins that do show reactivity to hydroxylamine, including the echidna<sup>23</sup> and the anole.<sup>24</sup> Variation has also been found in the kinetics of rhodopsin intermediates following photoactivation. Meta II rhodopsin decay rates in human<sup>26</sup> and bovine rhodopsin<sup>72</sup> are notably different from those in nonmammalian rhodopsins, such as chicken,<sup>49</sup> salamander,<sup>73</sup> and cichlid fish,<sup>62</sup> while meta III decay rates appear to be different even among mammalian rhodopsins.<sup>26</sup> These examples demonstrate how functional differences that mediate the disparity in rod and cone opsin properties may also show variation in different vertebrate rhodopsins. While these differences might not be of the same magnitude as those between rhodopsins and cone opsins, they reveal intriguing insights into the evolution of dim-light visual systems in vertebrates.

Although our study indicates that there are interesting differences in light-activated retinal release rates between zebrafish and bovine rhodopsin, the adaptive significance of this natural variation remains unclear. Since dark adaptation requires both release of all-*trans*-retinal from opsin following photoactivation, and regeneration of opsin with a new 11-*cis*-retinal chromophore, the rate of retinal release following light activation may affect the speed at which dark adaptation can occur. Under larger light bleaching conditions, the rate-limiting step of visual pigment regeneration is known to be related to the availability of new 11-*cis*-retinal in rod outer segments (ROS), and has been linked to either retinal isomerase activity in the retinal pigment epithelium (RPE),<sup>74</sup> or transport of newly metabolized 11-*cis*-retinal from the RPE to the ROS.<sup>75,76</sup> For small light bleaches, which may be more relevant under natural conditions, an existing pool of 11-*cis*-retinal in the ROS can regenerate 3–10% of visual pigments in the retina,<sup>77,78</sup> bypassing the rate-limiting activities involving the RPE and possibly leaving retinal release from rhodopsin as the rate-limiting factor.<sup>30</sup> It is also important when drawing associations to *in vivo* processes to consider that our experiments were performed in detergent, as membrane composition can influence rhodopsin kinetics.<sup>79,80</sup> Regardless, this remains an interesting avenue of research for both *in vivo* and *in vitro* comparative studies of vision.

■ ASSOCIATED CONTENT

● Supporting Information

Two-dimensional snake plot of zebrafish rhodopsin (Figure S1), retinal release data for bovine rhodopsin at 37 °C (Figure S2), and a sequence logo describing sequence variation among vertebrates at sites highlighted in this study that affect rates of retinal release (Figure S3). GenBank sequences used to generate Figure S3 (Table S1), and retinal release data for a reverse triple mutant in a bovine rhodopsin background (Table

S2). The Supporting Information is available free of charge on the ACS Publications website at DOI: 10.1021/bi501377b.

## AUTHOR INFORMATION

### Corresponding Author

\*Mailing address: Departments of Ecology & Evolutionary Biology/Cell & Systems Biology, University of Toronto, 25 Harbord Street, Toronto, Ontario M5S 3G5, Canada. Tel: 416-978-3507. Fax: 416-978-8532. E-mail: belinda.chang@utoronto.ca.

### Funding

This research was supported by a Natural Sciences and Engineering Research Council Discovery Grant (B.S.W.C.), and a University of Toronto Vision Science Research Program fellowship (J.M.M.).

### Notes

The authors declare no competing financial interest.

## ACKNOWLEDGMENTS

We acknowledge Vincent Tropepe for providing us with zebrafish genomic DNA and Amir Sabouhanian for help with homology modeling. We would like to thank two anonymous reviewers for their insightful comments and suggestions.

## ABBREVIATIONS

$\lambda_{MAX}$ , wavelength of maximum absorbance; cDNA, complementary deoxyribonucleic acid; DM, dodecyl maltoside; DNA, deoxyribonucleic acid; EL, extracellular loop; GPCR, G protein-coupled receptor; HEK293T, human embryonic kidney 293 cells with T antigen from simian virus 40; NaPhos, sodium phosphate;  $NH_2OH$ , hydroxylamine; PCR, polymerase chain reaction; RNA, ribonucleic acid; TM, transmembrane domain; VCOP, *Xenopus* short wavelength-sensitive cone opsin

## REFERENCES

- (1) Burns, M. E., and Baylor, D. A. (2001) Activation, deactivation, and adaptation in vertebrate photoreceptor cells. *Annu. Rev. Neurosci.* 24, 779–805.
- (2) Sakmar, T. P., Franke, R. R., and Khorana, H. G. (1989) Glutamic acid-113 serves as the retinylidene Schiff base counterion in bovine rhodopsin. *Proc. Natl. Acad. Sci. U. S. A.* 86, 8309–8313.
- (3) Corson, D. W., Cornwall, M. C., MacNichol, E. F., Jin, J., Johnson, R., Derguini, F., Crouch, R. K., and Nakanishi, K. (1990) Sensitization of bleached rod photoreceptors by 11-*cis*-locked analogues of retinal. *Proc. Natl. Acad. Sci. U. S. A.* 87, 6823–6827.
- (4) Pugh, E. N., and Lamb, T. D. (1993) Amplification and kinetics of the activation steps in phototransduction. *Biochim. Biophys. Acta* 1141, 111–149.
- (5) Gross, O. P., and Burns, M. E. (2010) Control of rhodopsin's active lifetime by arrestin-1 expression in mammalian rods. *J. Neurosci.* 30, 3450–3457.
- (6) Hofmann, K. P., Pulvermüller, A., Buczylo, J., Van Hooser, P., and Palczewski, K. (1992) The role of arrestin and retinoids in the regeneration pathway of rhodopsin. *J. Biol. Chem.* 267, 15701–15706.
- (7) Pulvermüller, A., Marezki, D., Rudnicka-Nawrot, M., Smith, W. C., Palczewski, K., and Hofmann, K. P. (1997) Functional differences in the interaction of arrestin and its splice variant, p44, with rhodopsin. *Biochemistry* 36, 9253–9260.
- (8) Palczewski, K., Kumasaka, T., Hori, T., Behnke, C. A., Motoshima, H., Fox, B. A., Le Trong, I., Teller, D. C., Okada, T., Stenkamp, R. E., Yamamoto, M., and Miyano, M. (2000) Crystal structure of rhodopsin: A G protein-coupled receptor. *Science* 289, 739–745.

(9) Park, J. H., Scheerer, P., Hofmann, K. P., Choe, H. W., and Ernst, O. P. (2008) Crystal structure of the ligand-free G-protein-coupled receptor opsin. *Nature* 454, 183–187.

(10) Choe, H. W., Kim, Y. J., Park, J. H., Morizumi, T., Pai, E. F., Krauss, N., Hofmann, K. P., Scheerer, P., and Ernst, O. P. (2011) Crystal structure of metarhodopsin II. *Nature* 471, 651–655.

(11) Okada, T., Sugihara, M., Bondar, A. N., Elstner, M., Entel, P., and Buss, V. (2004) The retinal conformation and its environment in rhodopsin in light of a new 2.2 Å crystal structure. *J. Mol. Biol.* 342, 571–583.

(12) Schädel, S. A., Heck, M., Marezki, D., Filipek, S., Teller, D. C., Palczewski, K., and Hofmann, K. P. (2003) Ligand channeling within a G-protein-coupled receptor. *J. Biol. Chem.* 278, 24896–24903.

(13) Wang, T., and Duan, Y. (2007) Chromophore channeling in the G-protein coupled receptor rhodopsin. *J. Am. Chem. Soc.* 129, 6970–6971.

(14) Scheerer, P., Park, J. H., Hildebrand, P. W., Kim, Y. J., Krauss, N., Choe, H. W., Hofmann, K. P., and Ernst, O. P. (2008) Crystal structure of opsin in its G-protein-interacting conformation. *Nature* 455, 497–502.

(15) Hildebrand, P. W., Scheerer, P., Park, J. H., Choe, H. W., Piechnick, R., Ernst, O. P., Hofmann, K. P., and Heck, M. (2009) A ligand channel through the G protein coupled receptor opsin. *PLoS One* 4, e4382.

(16) Farrens, D. L., Altenbach, C., Yank, K., Hubbell, W. L., and Khorana, H. G. (1996) Requirement of rigid-body motion of transmembrane helices for light activation of rhodopsin. *Science* 274, 768–770.

(17) Altenbach, C., Kusnetzow, A. K., Ernst, O. P., Hofmann, K. P., and Hubbell, W. L. (2008) High-resolution distance mapping in rhodopsin reveals the pattern of helix movement due to activation. *Proc. Natl. Acad. Sci. U. S. A.* 105, 7439–7444.

(18) Wang, T., and Duan, Y. (2011) Retinal release from opsin in molecular dynamics simulations. *J. Mol. Recognit.* 24, 350–358.

(19) Piechnick, R., Ritter, E., Hildebrand, P. W., Ernst, O. P., Scheerer, P., Hofmann, K. P., and Heck, M. (2012) Effect of channel mutations on the uptake and release of the retinal ligand in opsin. *Proc. Natl. Acad. Sci. U. S. A.* 109, 5247–5252.

(20) Chen, M. H., Kuemmel, C., Birge, R. R., and Knox, B. E. (2012) Rapid retinal release from a cone visual pigment following photo-activation. *Biochemistry* 51, 4117–4125.

(21) Liu, M. Y., Liu, J., Mehrotra, D., Liu, Y., Guo, Y., Baldera-Aguayo, P. A., Mooney, V. L., Nour, A. M., and Yan, E. C. (2013) Thermal Stability of Rhodopsin and Progression of Retinitis Pigmentosa: A Comparison of S186W and D190N Rhodopsin Mutants. *J. Biol. Chem.* 288, 17698–17712.

(22) Kuwayama, S., Imai, H., Morizumi, T., and Shichida, Y. (2005) Amino acid residues responsible for the meta-III decay rates in rod and cone visual pigments. *Biochemistry* 44, 2208–2215.

(23) Bickelmann, C., Morrow, J. M., Müller, J., and Chang, B. S. W. (2012) Functional characterization of the rod visual pigment of the echidna (*Tachygllossus aculeatus*), a basal mammal. *Visual Neurosci.* 29, 211–217.

(24) Kawamura, S., and Yokoyama, S. (1998) Functional characterization of visual and nonvisual pigments of American chameleon (*Anolis carolinensis*). *Vision Res.* 38, 37–44.

(25) Imai, H., Imamoto, Y., Yoshizawa, T., and Shichida, Y. (1995) Difference in molecular properties between chicken green and rod rhodopsin as related to the functional difference between cone and rod photoreceptor cells. *Biochemistry* 34, 10525–10531.

(26) Lewis, J. W., van Kujik, F. J., Carruthers, J. A., and Kliger, D. S. (1997) Metarhodopsin III formation and decay kinetics: comparison of bovine and human rhodopsin. *Vision Res.* 37, 1–8.

(27) Muto, A., Orger, M. B., Wehman, A. M., Smear, M. C., Kay, J. N., Page-McCaw, P. S., Gahtan, E., Xiao, T., Nevin, L. M., Gosse, N. J., Staub, W., Finger-Baier, K., and Baier, H. (2005) Forward genetic analysis of visual behavior in zebrafish. *PLoS Genet.* 1, e66.

(28) Fadool, J. M., and Dowling, J. E. (2008) Zebrafish: a model system for the study of eye genetics. *Prog. Retinal Eye Res.* 27, 89–110.

- (29) Maurer, C. M., Huang, Y. Y., and Neuhaus, S. C. (2011) Application of zebrafish oculomotor behavior to model human disorders. *Rev. Neurosci.* 22, 5–16.
- (30) Ala-Laurila, P., Kolesnikov, A. V., Crouch, R. K., Tsina, E., Shukolyukov, S. A., Govardovskii, V. I., Koutalos, Y., Wiggert, B., Estevez, M. E., and Cornwall, M. C. (2006) Visual cycle: dependence of retinol production and removal on photoproduct decay and cell morphology. *J. Gen. Physiol.* 128, 153–169.
- (31) Ferretti, L., Karnik, S. S., Khorana, H. G., Nassal, M., and Oprian, D. D. (1986) Total synthesis of a gene for bovine rhodopsin. *Proc. Natl. Acad. Sci. U. S. A.* 83, 599–603.
- (32) Morrow, J. M., and Chang, B. S. W. (2010) The p1D4-hrGFP II expression vector: a tool for expressing and purifying visual pigments and other G protein-coupled receptors. *Plasmid* 64, 162–169.
- (33) Molday, R. S., and MacKenzie, D. (1983) Monoclonal antibodies to rhodopsin: characterization, cross-reactivity, and application as structural probes. *Biochemistry* 22, 653–660.
- (34) Morrow, J. M., Lazic, S., and Chang, B. S. W. (2011) A novel rhodopsin-like gene expressed in zebrafish retina. *Visual Neurosci.* 28, 325–335.
- (35) Govardovskii, V. I., Fyhrquist, N., Reuter, T., Kuzmin, D. G., and Donner, K. (2000) In search of the visual pigment template. *Visual Neurosci.* 17, 509–528.
- (36) Farrens, D. L., and Khorana, H. G. (1995) Structure and function in rhodopsin. Measurement of the rate of metarhodopsin II decay by fluorescence spectroscopy. *J. Biol. Chem.* 270, 5073–5076.
- (37) Janz, J. M., Fay, J. F., and Farrens, D. L. (2003) Stability of dark state rhodopsin is mediated by a conserved ion pair in intradiscal loop E-2. *J. Biol. Chem.* 278, 16982–16991.
- (38) Sali, A., and Blundell, T. L. (1993) Comparative protein modeling by satisfaction of spatial restraints. *J. Mol. Biol.* 234, 779–815.
- (39) Eswar, N., Marti-Renom, M. A., Webb, B., Madhusudhan, M. S., Eramian, D., Shen, M., Pieper, U., and Sali, A. (2006) Comparative Protein Structure Modeling with MODELLER. *Current Protocols in Bioinformatics*, Supplement 15, 5.6.1–5.6.30, John Wiley & Sons, Inc., New York.
- (40) Shen, M. Y., and Sali, A. (2006) Statistical potential for assessment and prediction of protein structures. *Protein Sci.* 15, 2507–2524.
- (41) Laskowski, R. A., Moss, D. S., and Thornton, J. M. (1993) Main-chain bond lengths and bond angles in protein structures. *J. Mol. Biol.* 231, 1049–1067.
- (42) Wiederstein, M., and Sippl, M. J. (2007) ProSA-web: interactive web service for the recognition of errors in three-dimensional structures of proteins. *Nucleic Acids Res.* 35, W407–W410.
- (43) DeLano, W. L. (2008) *The PyMOL Molecular Graphics System*; DeLano Scientific LLC, Palo Alto, CA, <http://www.pymol.org>.
- (44) Oprian, D. D., Molday, R. S., Kaufman, R. J., and Khorana, H. G. (1987) Expression of a synthetic bovine rhodopsin gene in monkey kidney cells. *Proc. Natl. Acad. Sci. U. S. A.* 84, 8874–8878.
- (45) Chinen, A., Hamaoka, T., Yamada, Y., and Kawamura, S. (2003) Gene duplication and spectral diversification of cone visual pigments of zebrafish. *Genetics* 163, 663–675.
- (46) Menon, S. T., Han, M., and Sakmar, T. P. (2001) Rhodopsin: Structural basis of molecular physiology. *Physiol. Rev.* 81, 1659–1688.
- (47) Bowmaker, J. K. (2008) Evolution of vertebrate visual pigments. *Vision Res.* 48, 2022–2041.
- (48) Yan, E. C., Kazmi, M. A., De, S., Chang, B. S., Siebert, C., Marin, E. P., Mathies, R. A., and Sakmar, T. P. (2002) Function of extracellular loop 2 in rhodopsin: Glutamic acid 181 modulates stability and absorption wavelength of metarhodopsin II. *Biochemistry* 41, 3620–3627.
- (49) Imai, H., Kojima, D., Oura, T., Tachibana, S., Terakita, A., and Shichida, Y. (1997) Single amino acid residue as a functional determinant of rod and cone visual pigments. *Proc. Natl. Acad. Sci. U. S. A.* 94, 2322–2326.
- (50) Kuwayama, S., Imai, H., Hirano, T., Terakita, A., and Shichida, Y. (2002) Conserved proline residue at position 189 in cone visual pigments as a determinant of molecular properties different from rhodopsins. *Biochemistry* 41, 15245–15252.
- (51) Yan, E. C., Kazmi, M. A., Ganim, Z., Hou, J. M., Pan, D., Chang, B. S., Sakmar, T. P., and Mathies, R. A. (2003) Retinal counterion switch in the photoactivation of the G protein-coupled receptor rhodopsin. *Proc. Natl. Acad. Sci. U. S. A.* 100, 9262–9267.
- (52) Liu, J., Liu, M. Y., Nguyen, J. B., Bhagat, A., Mooney, V., and Yan, E. C. (2009) Thermal decay of rhodopsin: role of hydrogen bonds in thermal isomerization of 11-cis retinal in the binding site and hydrolysis of protonated Schiff base. *J. Am. Chem. Soc.* 131, 8750–8751.
- (53) Fahmy, K., Sakmar, T. P., and Siebert, F. (2000) Transducing-dependent protonation of glutamic acid 134 in rhodopsin. *Biochemistry* 39, 10607–10612.
- (54) Fritze, O., Filipek, S., Kuksa, V., Palczewski, K., Hofmann, K. P., and Ernst, O. P. (2003) Role of the conserved NPxxY(x)<sub>5,6</sub>F motif in the rhodopsin ground state and during activation. *Proc. Natl. Acad. Sci. U. S. A.* 100, 2290–2295.
- (55) Sakai, K., Imamoto, Y., Yamashita, T., and Shichida, Y. (2010) Functional analysis of the second extracellular loop of rhodopsin by characterizing split variants. *Photochem. Photobiol. Sci.* 9, 1490–1497.
- (56) Spence, R., Gerlach, G., Lawrence, C., and Smith, C. (2008) The behavior and ecology of the zebrafish *Danio rerio*. *Biol. Rev.* 83, 13–34.
- (57) Gain, A. K., Immerzeel, W. W., Sperna Weiland, F. C., and Bierkens, M. F. P. (2011) Impact of climate change on the stream flow of the lower Brahmaputra: trends in high and low flows based on discharge-weighted ensemble modeling. *Hydrol. Earth Syst. Sci.* 15, 1537–1545.
- (58) Fasicck, J. I., and Robson, P. R. (1998) Mechanism of spectral tuning in the dolphin visual pigments. *Biochemistry* 37, 433–438.
- (59) Hunt, D. M., Carvalho, L. S., Cowing, J. A., Parry, J. W., Wilkie, S. E., Davies, W. L., and Bowmaker, J. K. (2007) Spectral tuning of shortwave-sensitive visual pigments in vertebrates. *Photochem. Photobiol.* 83, 303–310.
- (60) Takenaka, N., and Yokoyama, S. (2007) Mechanisms of spectral tuning in the RH2 pigments of Tokay gecko and American chameleon. *Gene* 399, 26–32.
- (61) Bloch, N. I., Morrow, J. M., Chang, B. S. W., and Price, T. D. (2015) SWS2 visual pigment evolution as a test of historically contingent patterns of plumage color evolution in warblers. *Evolution* 69, 341–356.
- (62) Sugawara, T., Imai, H., Nikaido, M., Imamoto, Y., and Okada, N. (2010) Vertebrate rhodopsin adaptation to dim light via rapid meta-II intermediate formation. *Mol. Biol. Evol.* 27, 506–519.
- (63) Szundi, I., Epps, J., Lewis, J. W., and Kilger, D. S. (2010) Temperature dependence of the lumirhodopsin I-lumirhodopsin II equilibrium. *Biochemistry* 49, 5852–5858.
- (64) Korendayk, D. A., and Govardovskii, V. I. (2012) The effect of temperature on the slow stages of photolysis of rhodopsin in intact rods of frog and rat retinas. *Sens. Syst.* 26, 141–149.
- (65) Parkes, J. H., Gibson, S. K., and Liebman, P. A. (1999) Temperature and pH dependence of the metarhodopsin I-metarhodopsin II equilibrium and the binding of metarhodopsin II to G protein in rod disk membranes. *Biochemistry* 38, 6862–6878.
- (66) Shen, W. L., Kwon, Y., Adegbola, A. A., Luo, J., Chess, A., and Montell, C. (2011) Function of rhodopsin in temperature discrimination in *Drosophila*. *Science* 331, 1333–1336.
- (67) Liu, J., Liu, M. Y., Fu, L., Zhu, G. A., and Yan, E. C. (2011) Chemical kinetic analysis of thermal decay of rhodopsin reveals unusual energetics of thermal isomerization and hydrolysis of Schiff base. *J. Biol. Chem.* 286, 38408–38416.
- (68) Janz, J. M., and Farrens, D. L. (2004) Role of the retinal hydrogen bond network in rhodopsin Schiff base stability and hydrolysis. *J. Biol. Chem.* 279, 55886–55894.
- (69) Okano, T., Fukada, Y., Artamonov, I. D., and Yoshizawa, T. (1989) Purification of cone visual pigments from chicken retina. *Biochemistry* 28, 8848–8856.

(70) Johnson, R. L., Grant, K. B., Zankel, T. C., Boehm, M. F., Merbs, S. L., Nathans, J., and Nakanishi, K. (1993) Cloning and expression of goldfish opsin sequences. *Biochemistry* 32, 208–214.

(71) Starace, D. M., and Knox, B. E. (1998) Cloning and expression of a *Xenopus* short wavelength cone pigment. *Exp. Eye Res.* 67, 209–220.

(72) Yoshizawa, T., and Shichida, Y. (1982) Low-temperature spectrophotometry of intermediates of rhodopsin. *Method. Enzymol.* 81, 333–354.

(73) Das, J., Crouch, R. K., Ma, J. X., Oprian, D. D., and Kono, M. (2004) Role of the 9-methyl group of retinal in cone visual pigments. *Biochemistry* 43, 5532–5538.

(74) Lee, K. A., Nawrot, M., Garwin, G. G., Saari, J. C., and Hurley, J. B. (2010) Relationships among Visual Cycle Retinoids, Rhodopsin Phosphorylation, and Phototransduction in Mouse Eyes during Light and Dark Adaptation. *Biochemistry* 49, 2454–2463.

(75) Mahroo, O. A., and Lamb, T. D. (2004) Recovery of the human photopic electroretinogram after bleaching exposures: estimation of pigment regeneration kinetics. *J. Physiol (London, U. K.)* 554, 417–437.

(76) Lamb, T. D., and Pugh, E. N. (2006) Phototransduction, Dark Adaptation, and Rhodopsin Regeneration. *Invest. Ophthalm. Vis. Sci.* 47, 5138–5152.

(77) Azuma, L., Azuma, M., and Sickel, W. (1977) Regeneration of rhodopsin in frog outer segments. *J. Physiol.* 271, 747–759.

(78) Cocozza, J. D., and Ostroy, S. E. (1987) Factors affecting the regeneration of rhodopsin in the isolated amphibian retina. *Vision Res.* 27, 1085–1091.

(79) Litman, B. J., Kalisky, O., and Ottolenghi, M. (1981) Rhodopsin-phospholipid interactions: dependence of rate of the meta I to meta II transition on the level of associated disk phospholipid. *Biochemistry* 20, 631–634.

(80) Brown, M. F. (1994) Modulation of rhodopsin function by properties of the membrane bilayer. *Chem. Phys. Lipids* 73, 159–180.

(81) Crooks, G. E., Hon, G., Chandonia, J. M., and Brenner, S. E. (2004) WebLogo: A sequence logo generator. *Genome Res.* 14, 1188–1190.